Crystal structure under pressure of geometrically frustrated pyrochlores

Crystal structure under pressure of geometrically frustrated pyrochlores

A Apetrei[1], I Mirebeau[1], I Goncharenko[1] and W A Crichton[2]

[1] Laboratoire Léon Brillouin, CEA-CNRS, CE-Saclay, 91191 Gif-sur-Yvette, France
[2] European Synchrotron Radiation Facility, BP 220, 38043 Grenoble, France

E-mail: isabelle.mirebeau@cea.fr

Abstract

We have studied by x-ray synchrotron diffraction under high pressure five pyrochlore compounds: $Tb_2Ti_2O_7$ (up to 42 GPa), $Tb_2Sn_2O_7$ and $Tb_2Mo_2O_7$ (up to 35 GPa), $Gd_2Mo_2O_7$ and $(Tb_{0.8}La_{0.2})_2Mo_2O_7$ (up to 10 GPa). At ambient pressure all compounds crystallize in the cubic $Fd\bar{3}m$ symmetry group. This structure is stable for all compounds in the investigated pressure range. All three compounds having Mo as transition metal are described by the same equation of state, with the same bulk modulus $B_0 = 149$. The bulk modulus is smaller in the Mo pyrochlores than in the Ti and Sn ones, in contrast with *a priori* expectations.

1. Introduction

In pyrochlore oxides $R_2M_2O_7$ the rare earth ion R^{3+} and the transition or sp metal ion M^{4+} both occupy three-dimensional lattices of corner sharing tetrahedra. In recent years these systems have attracted great attention because their lattice can lead to geometrical frustration of the first neighbor magnetic interactions. Since such systems possess an enormous degeneracy of the ground state, they cannot order magnetically in a classical way. They show exotic magnetic ground states, short range ordered, which are called spin liquids, spin ices and spin glasses due to their striking similarities with the states of condensed matter [1]. In practice, the degeneracy of the ground state is generally lifted by a perturbation like pressure, which changes the energy balance between first neighbor exchange interaction, dipolar interaction and rare earth anisotropy and consequently induces new magnetic orders.

We first consider pyrochlores with non-magnetic M^{4+} ion, such as the 3d Ti^{4+} ion or the sp Sn^{4+} ion. These compounds are insulators and frustrated. Among them we studied those with R = Tb. $Tb_2Ti_2O_7$ is a well known example of a spin liquid where short range correlated magnetic moments fluctuate down to the lowest measured temperature of 70 mK [2]. Under applied pressure combined with stress it undergoes antiferromagnetic order [3, 4]. Replacing Ti by Sn yields a lattice expansion. Neutron diffraction measurements show that $Tb_2Sn_2O_7$ orders even at ambient pressure. It forms an 'ordered spin ice' state, coexisting with magnetic
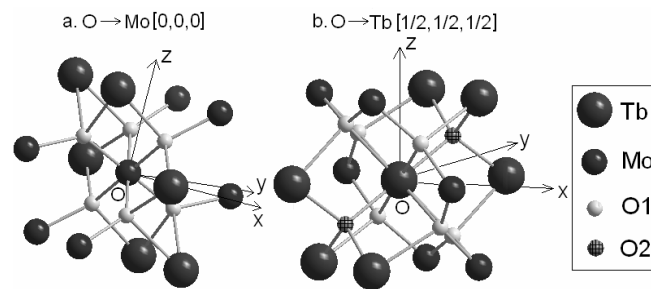
Figure 1. Crystal structure of $R_2M_2O_7$ showing the oxygen environment of an M^{4+} site (left) and an R^{3+} site (right). The structure is drawn for $Tb_2Mo_2O_7$.

fluctuations which persist down to the lowest temperatures [5–7]. Therefore, in $Tb_2Ti_2O_7$ and $Tb_2Sn_2O_7$, the variation of the interatomic distances under applied or chemical pressure changes the energy balance and induces very different magnetic ground states. It is important to know whether these effects are connected with changes in the crystal structure or oxygen position parameter, which can modify the superexchange interaction between Tb ions. This motivated the study of their crystal structure under pressure.

In $R_2Mo_2O_7$ pyrochlores where Mo^{4+} ions are magnetic, the variation of interatomic distances affects not only the magnetic but also the conduction properties. This variation may may be tuned by varying the mean ionic radius r of the rare earth R [8, 9]. Compounds with $r < r_C \sim 1.047$ Å (R = Y, Dy or Tb) are spin glasses and insulators (SGIs), whereas those with $r > r_C$ (R = Gd, Sm or Nd) show ferromagnetic metallic (FM) behavior. All $(RR')_2Mo_2O_7$ show the same variation of the magnetic properties and transition temperature versus the lattice constant, showing the dominant role of Mo–Mo interactions, although the influence of the rare earth cannot be excluded. Chemical pressure and applied pressure stabilize the spin glass state in the same way, as shown by the evolution of their magnetization [10–12], as well as by neutron and muon data [13–15]. However, their effects on the conduction properties are different, since the pressure induced spin glass state remains metallic [16]. This motivated our pressure study of the crystal structure in the critical region.

The crystal structure of $R_2M_2O_7$ pyrochlores of $Fd\bar{3}m$ symmetry is described as follows. The cubic unit cell of lattice constant a contains eight $R_2M_2O_7$ units, where R and M ions occupy two independent lattices of corner sharing tetrahedra. The oxygen environment is different for the R and M ions (figure 1). A given R^{3+} ion, corresponding to the 16d site $(1/2, 1/2, 1/2)$ of the $Fd\bar{3}m$ space group, is surrounded by six oxygen O1 (48f sites) with position $(3/8, 3/8, 1 - u)$ and equivalent positions, and two oxygen O2 (8b sites) with fixed positions $(3/8, 3/8, 3/8)$ and $(5/8, 5/8, 5/8)$. The R^{3+} oxygen environment is a puckered ring of six O1 ions with long R–O1 distances (2.54 Å in $Tb_2Mo_2O_7$) and a linear O2–R–O2 unit with short R–O2 distances (2.23 Å in $Tb_2Mo_2O_7$), normal to the average plane of the puckered ring. In contrast, the oxygen environment of a M^{4+} ion, on the 16c site $(0, 0, 0)$, consists of six oxygens O1 with equal M–O1 distances (2.01 Å in $Tb_2Mo_2O_7$). Besides the lattice constant a, the crystal structure is then controlled by the oxygen parameter u only. At ambient pressure the u values found for the pyrochlores studied here range between 0.32 and 0.34. They are intermediate between the value $u = 3/8 = 0.375$ corresponding to eight equal R–O distances for the R site and the value $u = 5/16 = 0.3125$ corresponding to a non-distorted octahedral environment for the M site.

The crystal structure of some $R_2M_2O_7$ pyrochlores was recently investigated under pressure by several groups. In $Gd_2Ti_2O_7$, Raman studies and and x-ray diffraction [17]

Table 1. Ambient pressure and temperature structural parameters of $R_2Mo_2O_7$ (R = Tb, Gd, (Tb, La)) and $Tb_2M_2O_7$ (M = Ti and Sn): the cubic lattice parameter a and positions of O 48f sites $[u, 1/8, 1/8]$. The bulk modulus B_0 as obtained from the fit using the Murnaghan equation (1) is also indicated. The pressure derivative of the bulk modulus was first fixed at $B_1 = 6$, when the fit takes into account the whole pressure range for all samples. Then we fixed $B_1 = 4.5$ and took into account the whole pressure range for $Tb_2Ti_2O_7$ and the 0–10 GPa interval for $R_2Mo_2O_7$ and $Tb_2Sn_2O_7$. The error bar on B_0, taking into account statistical and systematic errors, is estimated to be $\pm 3\%$.

Compound	a (Å) ambient pressure	u (units of a) ambient pressure	B_0 (GPa) $B_1 = 6$	B_0 (GPa) $B_1 = 4.5$
$Tb_2Mo_2O_7$	10.312(1)	0.334(3)	154	149
$Gd_2Mo_2O_7$	10.348(1)	0.334(1)	154	149
$(Tb_{0.8}La_{0.2})_2Mo_2O_7$	10.378(2)	0.331(1)	154	149
$Tb_2Ti_2O_7$	10.149(2)	0.328(2)	173	191
$Tb_2Sn_2O_7$	10.426(1)	0.336(1)	207	198

suggested a slight distortion at about 9 GPa. X-ray diffraction performed up to higher pressures [18, 19] concluded the presence of anion disorder in $Gd_2Ti_2O_7$ (above 38 GPa) and $Sm_2Ti_2O_7$ (above 40 GPa), and the onset of an amorphous phase above 51 GPa. In $Cd_2Nb_2O_7$, a pressure induced structural distortion from defect fluorite structure was found at 14 GPa, followed by a second transition towards monoclinic/orthorhombic then to amorphous state at about 27 GPa [21]. Similar results [20] were found in $Tb_2Ti_2O_7$ and $Tb_2Sn_2O_7$ with the first transition occurring at 51 and 37 GPa respectively, and the second one at 58 and 91 GPa, above the pressure range studied here. High pressure x-ray data were also obtained in $Nd_2Mo_2O_7$ up to 10 GPa [22].

Using high pressure x-ray synchrotron diffraction, we have studied five pyrochlore compounds and determined the equation-of-state parameters. First, for the same 4d transition metal M = Mo, we varied the rare earth ion and chose three compounds corresponding to the three regions of interest of the phase diagram: $Tb_2Mo_2O_7$ (in the SGI region, with $r < r_C$), $(Tb_{0.8}La_{0.2})_2Mo_2O_7$ (in the FM region, $r > r_C$) and $Gd_2Mo_2O_7$ (located on the verge of the transition, $r \sim r_C$). Then, vice versa, we fixed the rare earth R = Tb and compared $Tb_2Sn_2O_7$ with $Tb_2Ti_2O_7$ and $Tb_2Mo_2O_7$. By analyzing the crystal structure under pressure, we show that to the highest measured pressures there is no structural phase transition and that all compounds keep the ambient pressure cubic $Fd\overline{3}m$ symmetry group. The equation of state changes when changing the M metal (from sp to 3d and 4d). We also study the pressure dependence of the oxygen parameter u in all compounds.

2. Experimental details

All experiments were performed on powdered samples. Their crystal structure at ambient pressure was investigated by combining x-ray and neutron diffraction. Neutron diffraction measurements were performed on 3T2 ($Tb_2Sn_2O_7$ and $Tb_2Ti_2O_7$) and G61 ($Tb_2Mo_2O_7$ and $(Tb_{0.8}La_{0.2})_2Mo_2O_7$) diffractometers of the Laboratoire Léon Brillouin (LLB). Due to the huge absorption of natural Gd, neutron experiments on $Gd_2Mo_2O_7$ were done using a isotopically enriched ^{160}Gd and the high resolution–high flux diffractometer D2B of the Institute Laüe Langevin (ILL). The structural parameters at ambient pressure are given in table 1. X-ray synchrotron diffraction measurements under pressure at ambient temperature were performed on the ID27 beam line of the European Synchrotron Radiation Facility (ESRF). The incident wavelength was $\lambda = 0.3738$ Å. We used a diamond-anvil cell. The transmitting
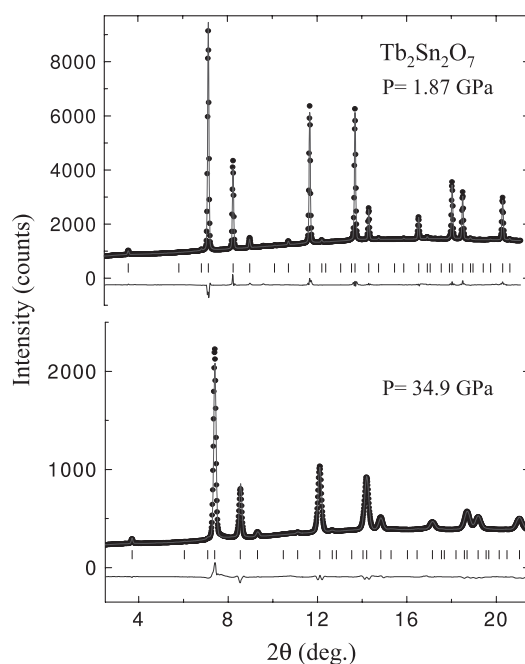
Figure 2. $Tb_2Sn_2O_7$: x-ray diffraction intensity versus the scattering angle 2θ at ambient temperature at $P = 1.87$ and 31.8 GPa, respectively. The incident x-ray wavelength is $\lambda = 0.3738$ Å. Solid lines show the best Rietveld refinement with cubic $Fd\overline{3}m$ symmetry ($R_B = 6.09\%$ and 6.91%, respectively) and the difference spectrum (bottom). Tick marks show the Bragg peak positions.

medium and the maximal pressure are as follows: $Tb_2Mo_2O_7$ (nitrogen, $P_{max} = 35$ GPa), $Gd_2Mo_2O_7$ (ethanol–methanol mixture, $P_{max} = 10$ GPa), $(Tb_{0.8}La_{0.2})_2Mo_2O_7$ (ethanol–methanol mixture, $P_{max} = 10$ GPa), $Tb_2Ti_2O_7$ (neon, $P_{max} = 42$ GPa) and $Tb_2Sn_2O_7$ (ethanol–methanol mixture, $P_{max} = 35$ GPa).

For $Tb_2M_2O_7$ (M = Mo, Ti or Sn) we went to higher pressures in order to compare the effects of M substitution on the equation of state. Per contra, for the other two molybdenum pyrochlores ($Gd_2Mo_2O_7$ and $(Tb_{0.8}La_{0.2})_2Mo_2O_7$) we used a maximum pressure of 10 GPa, which goes well beyond the F–SG transition.

3. Results

The crystal structure at ambient and under applied pressure was determined by Rietveld refinements of x-ray and neutron diffraction patterns, using the crystallographic programs of the FullProf suite [23]. Refinements of ambient pressure patterns show that all samples crystallize in the $Fd\overline{3}m$ space group, yielding a lattice parameter a and an oxygen position parameter u as indicated in table 1.

Under pressure, to the highest pressure value, there is a peak broadening, but neither additional peaks nor a splitting of the existing ones. This shows that the crystal structure remains cubic with $Fd\overline{3}m$ space group in the whole pressure range.

Figure 2 shows two x-ray diffraction patterns of $Tb_2Sn_2O_7$ at ambient temperature for two typical pressures, in the low and high pressure ranges. It clearly shows that there is no structural phase transition.
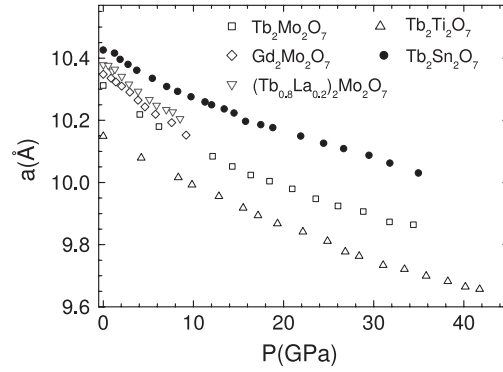
Figure 3. Variation of the lattice parameter *a* deduced from the structural analysis, versus pressure at ambient temperature for the five samples: $Tb_2Mo_2O_7$ ($\square$), $Gd_2Mo_2O_7$, ($\diamond$), $(Tb_{0.8}La_{0.2})_2Mo_2O_7$ ($\triangledown$), $Tb_2Ti_2O_7$ ($\triangle$) and $Tb_2Sn_2O_7$ ($\bullet$).

The evolution of the structural parameters *a* and *u* with pressure was determined as follows. For each sample we made the following analysis. First we fitted some selected Bragg peaks, yielding the pressure dependence of *a* only but with high accuracy. Then we analyzed the whole patterns using Fullprof in the profile matching mode, with no constraint on the peak intensities. Finally, we performed a structure analysis with Fullprof, allowing the determination of both *a* and *u*. A Thompson–Cox–Hastings pseudo-Voigt peak shape function was used (for details see [23, 24]). The determinations of *a* agree for the three analyses. Its evolution with pressure is shown in figure 3 for all samples.

The equation of state was determined by fitting the Murnaghan equation to the data:

$$\frac{V}{V_0} = \left(P \frac{B_1}{B_0} + 1 \right)^{-\frac{1}{B_1}} \tag{1}$$

with V_0, B_0 and B_1 the volume at zero pressure, the bulk modulus and its first pressure derivative, respectively.

In a first step, when fitting, we took into account the whole experimental pressure range for all samples, no matter what the pressure transmitting medium. We performed systematic fits using different values for the first pressure derivative of the bulk modulus, B_1. Then we fixed the value $B_1 = 6$, which allows a reasonable fit for all samples in the whole pressure range. As clearly seen in figure 4, for $R_2Mo_2O_7$ the variation of V/V_0 versus pressure is independent of the mean ionic radius of the rare earth *r*. $Tb_2Mo_2O_7$ ($r < r_C$), $Gd_2Mo_2O_7$ ($r \sim r_C$) and $(Tb_{0.8}La_{0.2})_2Mo_2O_7$ ($r > r_C$) are described by the same equation of state. The values of the bulk modulus B_0 deduced from this fit are listed in 1.

The high B_1 value found in the above analysis may reflect some non-hydrostaticity above 10 GPa, considering the fact that different transmitting media were used, and only neon is believed to be fully hydrostatic at high pressure. The non-hydrostaticity of nitrogen (used for $Tb_2Sn_2O_7$) and ethanol–methanol (used for $Tb_2Mo_2O_7$) with respect to neon (used for $Tb_2Ti_2O_7$) is confirmed by a strong increase of the peak width above 10 GPa, as shown by the pressure dependence of the parameter *Y* (inset of figure 5), which corresponds to the Lorentzian component of the Thompson–Cox–Hastings pseudo-Voigt peak shape function [23, 24]. This prevents giving a physical meaning to the high B_1 value. So in a second step, we took as reference $Tb_2Ti_2O_7$ measured with the neon transmitting medium. As shown in figure 5, a good fit of the $Tb_2Ti_2O_7$ data can be obtained with a more reasonable value of the bulk modulus derivative, $B_1 = 4.5$. An independent fit of B_0 and B_1 yields the values $B_0 = 187$ GPa and
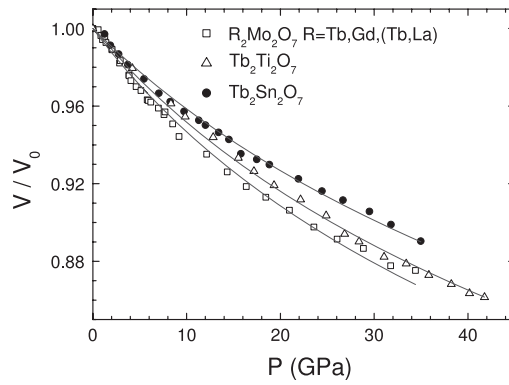
Figure 4. Pressure dependence of V/V_0, with V_0 the unit cell volume at ambient pressure. Lines correspond to fits using the Murnaghan function with fixed $B_1 = 6$ in the whole pressure range for all samples. The corresponding values of B_0 are indicated in table 1.
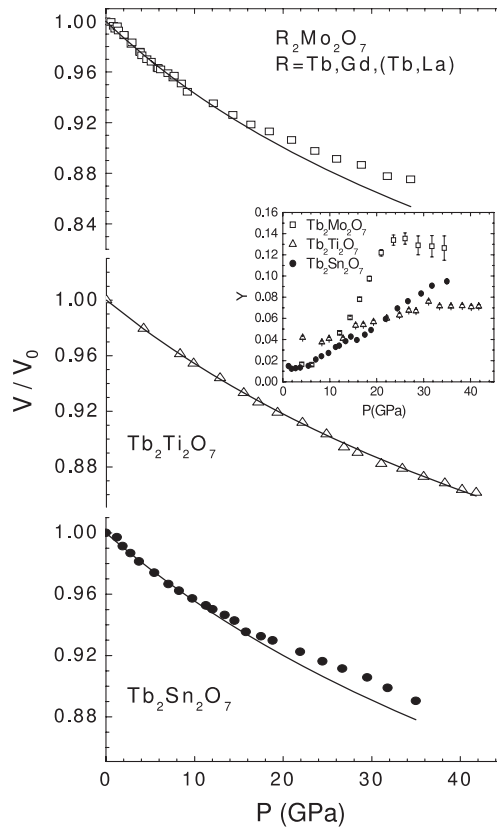

Figure 5. Pressure dependence of V/V_0. Lines correspond to fits using the Murnaghan function. The bulk modulus was fixed: $B_1 = 4.5$. For $Tb_2Ti_2O_7$ the fit was done in the whole pressure range, while for $R_2Mo_2O_7$ and $Tb_2Sn_2O_7$ the fit corresponds to the 0–10 GPa interval. The corresponding values of B_0 are also indicated in table 1, last column. Inset, the variation of the parameter Y, related to the intrinsic peak width, with pressure. Data for $Tb_2Ti_2O_7$ are the only ones which correspond to a fully hydrostatic pressure in the whole pressure range.
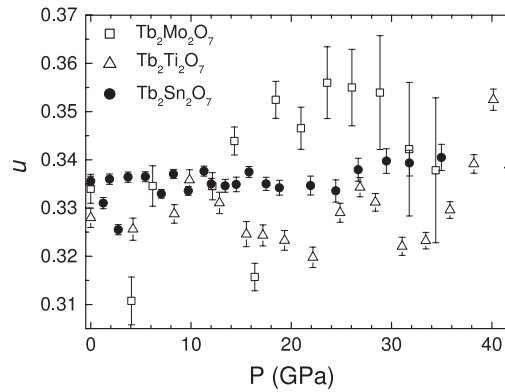
Figure 6. Oxygen position parameter u versus pressure at ambient temperature for Tb pyrochlores: $Tb_2Mo_2O_7$ ($\square$), $Tb_2Ti_2O_7$ ($\triangle$) and $Tb_2Sn_2O_7$ ($\bullet$).

$B_1 = 4.8$. We then fitted the data of the other samples, $R_2Mo_2O_7$ and $Tb_2Sn_2O_7$, by fixing $B_1 = 4.5$ and limiting the fitted pressure range to 10 GPa, an interval where ethanol–methanol mixture or nitrogen provide hydrostatical pressure conditions. The corresponding values of B_0 are listed in table 1, last column. We consider these values as the most reliable, since they fit well the $Tb_2Ti_2O_7$ data in the whole pressure range and also the region of interest 0–10 GPa of the molybdenum pyrochlores. Therefore we used them in the following to obtain the equation of state.

As shown in table 1, the bulk modulus increases in the sequence $B_0(Mo) < B_0(Ti) < B_0(Sn)$. This remains true whatever the value fixed for B_1.

The determination of the oxygen coordinate u is more intricate. It is directly related to the integrated intensities of the Bragg peaks, which may be partly affected by either texture effects or non-isotropic powder averaging for very small samples. Since it is the only structural parameter (besides a), we still obtained reasonable values (figure 6). For each sample, the average u value agrees with the ambient pressure determination within less than $\pm 1\%$. The influence of the scatter in u values on the determination of the interatomic distances for a given sample under pressure is evaluated in the worst case ($Tb_2Mo_2O_7$). For $a = 10.112$ Å ($Tb_2Mo_2O_7$ at 10 GPa), the scatter in u of 0.33(1) corresponds to a d (Mo–O1) distance of 1.96(4) Å and an Mo–O1–Mo angle of 131(5)°.

In figure 6, the oxygen coordinate u is shown versus pressure when varying the metal, M = Mo, Ti and Sn. In each case u is independent of applied pressure in the error bar limits. The u values for $Tb_2Ti_2O_7$ are systematically lower than for $Tb_2Sn_2O_7$, whereas the value for $Tb_2Mo_2O_7$ seems to be slightly higher. Our results for Ti and Sn samples agree with previous results [20], which show that the cubic crystal structure is stable and u is independent of pressure in this pressure range.

Figure 7 shows the evolution of u with the lattice constant for the Mo pyrochlore samples: $Tb_2Mo_2O_7$ ($a < a_c \sim 10.33$ Å), $Gd_2Mo_2O_7$ ($a \sim a_c$) and $(Tb_{0.8}La_{0.2})_2Mo_2O_7$ ($a > a_c$), in the pressure range 0–10 GPa. A pressure of 10 GPa is well beyond the values needed to induce the F–SG transition for both Gd and $(Tb_{0.8}La_{0.2})_2Mo_2O_7$ samples, where the critical pressure lies in the range 0.6–2.4 GPa ([14] and references therein) and around 2.1 GPa [13], respectively. The threshold pressures correspond to a critical value of the lattice constant $a_c \sim 10.33$ Å. Within the accuracy of our measurements we cannot evidence any systematic variation of u throughout the threshold. Our results are reported together with ambient pressure data on several samples
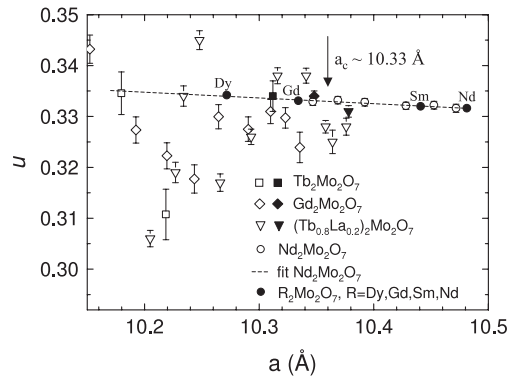
Figure 7. Oxygen coordinate against lattice parameter for the three Mo pyrochlores: $Tb_2Mo_2O_7$, $Gd_2Mo_2O_7$ and $(Tb_{0.8}La_{0.2})_2Mo_2O_7$. Open symbols ($\square$, $\diamond$, $\triangledown$) correspond to data under pressure, while the solid symbols indicate the ambient pressure data. For comparison the behavior of $Nd_2Mo_2O_7$ ($\bigcirc$) under applied pressure is shown, as cited from [22]. The dashed line is a linear fit of these data. The effect of rare earth substitution as in [9] is also shown ($\bullet$). a_c is the critical value of the lattice constant as in [13, 14].

with mean ionic radius encompassing the threshold (our data and from [9], as well as high pressure x-ray data on $Nd_2Mo_2O_7$ obtained up to 10 GPa [22]), where the powder averaging seems to be better than here. Our determination of u is situated in the expected range. The very small increase observed under chemical pressure and in [22] (the dashed line in figure 5 corresponds to an increase from 0.3315 to 0.3348, namely about 1% when a varies from 10.5 to 10.2 Å) is beyond the accuracy of the present pressure data.

4. Discussion

The determination of the crystal structure under pressure in rare earth pyrochlores is important since it governs their magnetic and electric properties, which strongly vary under pressure. In all samples, we find that the cubic structure with $Fd\bar{3}m$ symmetry is stable up to the highest measured pressure of 40 GPa, in agreement with previous results.

Considering the good stability of the crystal structure, the only parameters are the lattice constant a and oxygen parameter u. The determination of the equation of state $a(P)$ shows that the bulk modulus B_0 changes when changing the sp or d ion, whereas it does not change with the rare earth ion. One naturally expects that a change in the R ion should have much smaller effects on B_0 than a change in the sp or d ion, since the changes in the atomic radius are smaller, and the localized 4f shells do not participate in the atomic bonding.

We first consider the $Tb_2M_2O_7$ pyrochlores (M = Sn, Ti, Mo). One notices that $Tb_2Mo_2O_7$ has a larger unit cell than $Tb_2Ti_2O_7$, and also the smallest value of the bulk modulus of all compounds. This is not *a priori* expected from the variation of the ionic radius, evaluated in the periodic table as 0.71, 0.68 and 0.68 for Sn^{4+}, Ti^{4+} and Mo^{4+} ions respectively. The softening observed for the Mo compound may be related to the proximity of an insulating–metal transition [25, 26].

The oxygen parameter $\langle u \rangle$, averaged in the range 0–40 GPa, decreases from 0.335(2) for Sn to 0.325(3) for Ti. The decrease of $\langle u \rangle$ corresponds to a decrease of the trigonal compression of the oxygen octahedra around the M atom along the $\langle 111 \rangle$ axis, (the non-distorted case yielding $u = 5/16 = 0.312$). In [22], the small increase of u under applied pressure was explained by the fact that with decreasing a the MO_6 octahedron should become more trigonally

8

compressed, the O1 oxygen on the 48f sites going away from the Mo tetrahedron to compensate the volume compression. This argument obviously does not hold for chemical pressure induced by Ti/Sn substitution. One also notices that the substitution of Sn by Ti corresponds to chemical pressures of about 7 and 21 GPa respectively, well below the maximum pressures investigated. So the decrease of u when going from Sn to Ti may arise from another reason than the lattice contraction. The influence of the crystal field of the Tb^{3+} ion, which is strongly different in the Ti and Sn compounds [27], could play a role.

We then consider the $R_2Mo_2O_7$ pyrochlores, when we vary the rare earth ion. Here the variations of both B_0 and $\langle u \rangle$ are much smaller and beyond the accuracy of our measurements. We find the same equation of state on both sides of the SG–F threshold, and we did not observe any variation u either under pressure, within the accuracy of our measurements. A very small systematic variation of u with a ($\sim 1\%$ within the whole $R_2Mo_2O_7$ family) is found at ambient pressure under chemical substitution [9] and in the high pressure data of [22]. Our neutron diffraction data on $(Tb_{1-x}La_x)_2Mo_2O_7$ samples, to be published later, where we investigated the threshold region in details at ambient pressure, confirm this effect. The small variation of u scales with a in a unique curve for all rare earth ions. The change in the Mo–O–Mo bond angle is about negligible in the threshold region.

This suggests that the only structural parameter which controls the ferromagnetic–spin glass and insulating–metal transition, or at least the change in sign of the Mo–Mo magnetic interactions, is the Mo–Mo distance and not the Mo–O–Mo bond angle. This result may be considered with regards to band structure calculations. In [28], the stability of the ferromagnetic phase was related to the variation of the bond angle. Our data rather support the picture of [29], which argues that the key parameter in this transition is not the Mo–O–Mo angle, which controls $Mo(t_{2g})$ orbitals mediated by O(2p) states, but the Mo–Mo distance, directly related to the lattice constant, which controls the direct interactions between the extended Mo (4d) orbitals.

5. Conclusion

By means of high pressure x-ray synchrotron diffraction we have studied the crystal structure of $Tb_2Mo_2O_7$, $Gd_2Mo_2O_7$, $(Tb_{0.8}La_{0.2})_2Mo_2O_7$, $Tb_2Ti_2O_7$ and $Tb_2Sn_2O_7$ pyrochlore compounds. We have shown that there is no structural phase transition to the highest applied pressure. The pressure dependence of lattice and oxygen position parameters was investigated since these two parameters determine the crystal structure and hence the electronic and magnetic properties of the pyrochlores. In $Tb_2M_2O_7$ (M = Mo, Ti, Sn) the bulk modulus increases when varying the transition metal from Mo to Ti and then to the sp metal Sn. In contrast, $R_2Mo_2O_7$ pyrochlores are all described by the same equation of state, whatever their electric or low temperature magnetic state.

References

[1] Greedan J E 2001 *J. Mater. Chem.* **11** 37
[2] Gardner J S, Dunsiger S R, Gaulin B D, Gingras M J P, Greedan J E, Kiefl R F, Lumsden M D, MacFarlane W A, Raju N P, Sonier J E, Swainson I and Tun Z 1999 *Phys. Rev. Lett.* **82** 1012

 [3] Mirebeau I, Goncharenko I N, Cadavez-Peres P, Bramwell S T, Gingras M J P and Gardner J S 2002 *Nature*
       420 54
 [4] Mirebeau I, Goncharenko I, Dhalenne G and Revcolevschi A 2004 *Phys. Rev. Lett.* **93** 187204
 [5] Mirebeau I, Apetrei A, Rodríguez-Carvajal J, Bonville P, Forget A, Colson D, Glazkov V, Sanchez J P,
       Isnard O and Suard E 2005 *Phys. Rev. Lett.* **94** 246402
 [6] Bert F, Mendels P, Olariu A, Blanchard N, Collin G, Amato A, Baines C and Hillier A D 2006 *Phys. Rev. Lett.*
       97 117203
 [7] Dalmas de Réotier P, Yaouanc A, Keller L, Cervellino A, Roessli B, Baines C, Forget A, Vaju C,
       Gubbens P C M, Amato A and King P J C 2006 *Phys. Rev. Lett.* **96** 127202
 [8] Katsufuji T, Hwang H Y and Cheong S-W 2000 *Phys. Rev. Lett.* **84** 1998
 [9] Moritomo Y, Xu S, Machida A, Katsufuji T, Nishibori E, Takata M, Sakata M and Cheong S W 2001 *Phys. Rev.*
       B **63** 144425
[10] Park J G, Jo Y, Park J, Kim H C, Ri H C, Xu S, Moritomo Y and Cheong S W 2003 *Physica* B **328** 90
[11] Kim H C, Jo Y, Park J G, Ri H C and Cheong S W 2003 *Acta Phys. Pol.* B **34** 1429
       Kim H C, Jo Y, Park J G, Ri H C and Cheong S W 2005 *Physica* B **359** 1246
[12] Miyoshi K, Takamatsu Y and Takeuchi J 2006 *J. Phys. Soc. Japan* **75** 065001
[13] Apetrei A, Mirebeau I, Goncharenko I, Andreica D and Bonville P 2006 *Phys. Rev. Lett.* **97** 206401
[14] Mirebeau I, Apetrei A, Goncharenko I, Andreica D, Bonville P, Sanchez J P, Amato A, Suard E and Crichton W
       2006 *Phys. Rev.* B **74** 174414
[15] Apetrei A, Mirebeau I, Goncharenko I, Andreica D and Bonville P 2007 *J. Phys.: Condens. Matter* **19** 145214
[16] Miyoshi K, Yamashita T, Fujiwara K and Takeuchi J 2003 *J. Phys. Soc. Japan* **72** 1855
[17] Saha S, Muthu D V S, Pascanut C, Dragoe N, Suryanarayanan R, Dhalenne G, Revcolevschi A, Karmakar S,
       Sharma S M and Sood A K 2006 *Phys. Rev.* B **74** 064109
[18] Zhang F X, Manoun B, Saxena S K and Zha C S 2005 *Appl. Phys. Lett.* **86** 181906
[19] Zhang F X and Saxena S K 2005 *Chem. Phys. Lett.* **413** 248
[20] Kumar R S, Cornelius A L, Nicol M F, Kham K C, Cheetham A C and Gardner J S 2006 *Appl. Phys. Lett.*
       88 031903
[21] Zhang F X, Lian J, Becker U, Ewing R C, Wang L M, Boatner L A, Hu J and Saxena S K 2006 *Phys. Rev.* B
       74 174116
[22] Ishikawa H, Xu Sh, Moritomo Y, Nakamura A, Ohishi Y and Kato K 2004 *Phys. Rev.* B **70** 104103
[23] Rodríguez-Carvajal J 1993 *Physica* B **192** 55
       For a recent version of FullProf, see Rodríguez-Carvajal J 2001 *CPD Newslett.* **26** 12 available at http://journals.
       iucr.org/iucr-top/comm/cpd/newsletters
[24] Finger L W, Cox D E and Jephcoat A P 1994 *J. Appl. Crystallogr.* **27** 892
[25] Kesmarki I, Hanasaki N, Hashimoto D, Iguchi S, Miyasakoa S and Tokura Y 2003 *Phys. Rev. Lett.* **67** 174406
[26] Kim M W, Lee Y S, Noh T W, Yu J and Moritomo Y 2004 *Phys. Rev. Lett.* **92** 27202
[27] Mirebeau I, Bonville P and Hennion M 2007 *Phys. Rev.* B submitted
[28] Kang J-S, Moritomo Y, Xu S H, Olson C G, Park J H, Kwon S K and Min B I 2002 *Phys. Rev.* B **65** 224422
[29] Solovyev I V 2003 *Phys. Rev.* B **67** 174406